Structural Engineering and Mechanics, *Vol. 70, No. 5 (2019) 535-549*
DOI: https://doi.org/10.12989/sem.2019.70.5.535

Numerical analysis for free vibration of hybrid laminated composite plates for different boundary conditions

Mohammed Amine Benhenni[1,2], Tahar Hassaine Daouadji[2], Boussad Abbès*[1], Fazilay Abbès[1], Yuming Li[1] and Belkacem Adim[2]

[1]*GRESPI – University of Reims , Campus du Moulin de la Housse BP 1039 - 51687 Reims cedex 2, France.*
[2]*Laboratoire de Géomatique et Développement Durable, University of Tiaret, Algeria*

(Received July 12, 2018, Revised March 5, 2019, Accepted March 8, 2019)

Abstract. This study aimed to develop a high-order shear deformation theory to predict the free vibration of hybrid cross-ply laminated plates under different boundary conditions. The equations of motion for laminated hybrid rectangular plates are derived and obtained by using Hamilton's principle. The closed-form solutions of anti-symmetric cross-ply and angle-ply laminates are obtained by using Navier's solution. To assess the validity of our method, we used the finite element method. Firstly, the analytical and the numerical implementations were validated for an antisymmetric cross-ply square laminated with available results in the literature. Then, the effects of side-to-thickness ratio, aspect ratio, lamination schemes, and material properties on the fundamental frequencies for different combinations of boundary conditions of hybrid composite plates are investigated. The comparison of the analytical solutions with the corresponding finite element simulations shows the good accuracy of the proposed analytical closed form solution in predicting the fundamental frequencies of hybrid cross-ply laminated plates under different boundary conditions.

Keywords: composites; finite element method (FEM); laminates; plate/shell structures; frequency/modal analysis

1. Introduction

In recent years, laminated composite plates made have been using intensively in many engineering applications such as aerospace, automobile, shipbuilding and civil infrastructures, thanks to their high strength and stiffness, low weight, and durability. To use the laminated composite plates optimally, it is necessary to develop appropriate analysis theories to predict precisely their structural and dynamical behavior. Several mathematical models have been proposed in the literature (Reddy 1997). The classical laminated plate theory (CLPT) is the first model used to determine the stresses and deformations in plates subjected to external loading. In this theory, the transverse shear effects are neglected limiting its application to thin plates only. The first-order shear deformation theory (FSDT) is the first alternative proposed by Mindlin (1951) taking into account shear deformations through the thickness of isotropic plates. This theory was generalized to laminated anisotropic plates by Stavski(1965). However, Whitnay (1973) showed that the first-order shear deformation theory does not satisfy the equilibrium conditions at the top and bottom faces of the plate; and that shear correction factors are required to correct the unrealistic variation of the shear strains and stresses through the plate thickness. To overcome these limitations, high-order shear deformation theories, involving higher-order terms in Taylor's expansions of the displacements through the plate thickness, were proposed (Reddy 1984a, Reddy 1984b, Reddy 1990, Ren 1990, Benhenni 2018, Belkacem 2016, Adim 2018, Zenkour 2006, Mantari 2012, Mahi 2015, Adim 2016a, Adim 2016b, Hassaine Daouadji 2017, Hassaine Daouadji 2016a, Abdelhak 2016, Abualnour 2016, Abdelaziz 2017,Attia 2018, Belabed 2018, Bellifa 2017, Beldjillali 2016, Benchohra 2018, Benouna 2016, Boukhari 2016, Bousahla 2016, Draiche 2016, Bouderba 2016, Elhaina 2017, Fourn 2018, Hadji 2016, Hadji 2017, Hadji 2019a, Hadji 2019b, Houari 2016, Kaci 2018, Karami 2018, Khalifa 2018, Menasria 2017, Sobhy 2013, Tounsi 2013, Yazid 2018, Younsi 2018, Zohra 2016, Zouatnia 2018, Bennoun 2016, Benferhat 2016a, Hassaine Daouadji 2016b, Benferhat 2016b, Tu *et al*. 2017, Javed 2018, Rabia 2016a, Rabia 2016b, Tahar 2016a, Tahar 2016b, Tahar 2016c,Yousfi 2018). The key features of these theories are that they do not require shear correction factor and are similar to the classical plate theory in some aspects such as governing equation, boundary conditions and moment expressions.

In the development of modern composite materials, the manufacturers need to satisfy diverse and contradictory requirements, in which a combination of reinforcing layers from two or more types of fibers can overcome, leading to the so-called hybrid composite materials. Such an approach allows the simultaneous realization of the advantages of heterogeneous composites and the elimination of their undesirable characteristics. The hybrid fiber reinforced composites enhance the mechanical, thermal and damping among other properties compared to single-fiber reinforced composites (Sathishkumar *et al*. 2014). One application of

*Corresponding author, Ph.D.
E-mail: boussad.abbes@univ-reims.fr

ISSN: 1225-4568 (Print), 1598-6217 (Online)

these materials is associated with the so-called thermo-stable structures that do not change their dimensions under heating or cooling.

In this paper, a refined shear deformation theory of plates for the free vibration study of hybrid laminated composite plates is presented. Closed-form solutions of antisymmetric cross-ply hybrid laminates under different boundary conditions are obtained. The results are validated with existing results in the literature and with results obtained using the commercial finite element code ABAQUS.

2. Elastic properties of hybrid lamina

Hybrid laminated composite plates consisting of two different fibers as carbon/glass, glass/aramid and so on are considered in this study. The mechanical properties of these materials depend on fibers and matrix whose quantities in the materials are specified by volume and mass fractions. The effective elastic properties of this kind of lamina are given by the following equations (Vasiliev and Morozov 2001):

$$E_1 = E_f^{(1)}V_f^{(1)} + E_f^{(2)}V_f^{(2)} + E_m V_m \tag{1}$$

where E_1 is the longitudinal effective modulus, $E_f^{(1)}$ and $E_f^{(2)}$ are Young's moduli of the fibers of the first and of the second type, E_m is the matrix Young's modulus, $V_f^{(1)}$ and $V_f^{(2)}$ are volume fractions of the fibers of the first and of the second type and V_m is the matrix volume fraction, so that:

$$V_f^{(1)} + V_f^{(2)} + V_m = 1 \tag{2}$$

$$V_f = V_f^{(1)} + V_f^{(2)} \tag{3}$$

where V_f is the total volume fraction of the fibers.

And the normalized volume fractions of fibers are defined as:

$$w_f^{(1)} = \frac{V_f^{(1)}}{V_f},\ w_f^{(2)} = \frac{V_f^{(2)}}{V_f} \tag{4}$$

so that:

$$E_1 = V_f\left[E_f^{(1)}w_f^{(1)} + E_f^{(2)}\left(1-w_f^{(1)}\right)\right] + E_m\left(1-V_f\right) \tag{5}$$

The in-plane effective Poisson's coefficient of the hybrid laminated composite ν_{12} can be calculated by:

$$\nu_{12} = V_f\left[\nu_f^{(1)}w_f^{(1)} + \nu_f^{(2)}\left(1-w_f^{(1)}\right)\right] + \nu_m\left(1-V_f\right) \tag{6}$$

where $\nu_f^{(1)}$ and $\nu_f^{(2)}$ are Poisson's coefficients of the fibers of the first and of the second type, ν_m is the matrix Poisson's coefficient.

The shear moduli of the fibers and the matrix are given by:

$$G_f^{(1)} = \frac{E_f^{(1)}}{2\left(1+\nu_f^{(1)}\right)},\quad G_f^{(2)} = \frac{E_f^{(2)}}{2\left(1+\nu_f^{(2)}\right)}, \tag{7}$$

$$G_m = \frac{E_m}{2\left(1+\nu_m\right)}$$

where $G_f^{(1)}$ and $G_f^{(2)}$ are shear moduli of the fibers of the first and of the second type, G_m is the matrix shear modulus.

The total effective modulus of the fibers is given by:

$$G_f = G\nu_f^{(1)}w_f + G_f^{(2)}\left(1-w_f\right) \tag{8}$$

The compressibility moduli of the fibers and the matrix are given by:

$$k_f = \frac{E_f^{(1)}w_f}{3\left(1-2\nu_f^{(1)}\right)} + \frac{E_f^{(2)}w_f}{3\left(1-2\nu_f^{(2)}\right)},\quad k_m = \frac{E_m}{3\left(1-2\nu_m\right)} \tag{9}$$

The lateral compressibility modulus of the fibers and the matrix are given respectively by:

$$K_f = k_f + \frac{G_f}{3},\quad K_m = k_m + \frac{G_m}{3} \tag{10}$$

The effective shear in-plane and out-of-plane moduli of the composite plate are then given by:

$$\begin{cases} G_{12} = G_{13} = G_m\dfrac{G_f\left(1+V_f\right)+G_m\left(1-V_f\right)}{G_f\left(1-V_f\right)+G_m\left(1+V_f\right)} \\ G_{23} = G_m\left(1+\dfrac{V_f}{\dfrac{G_m}{G_f-G_m}+\left(1-V_f\right)\dfrac{k_m+\frac{7}{3}G_m}{2k_m+\frac{8}{3}G_m}}\right) \end{cases} \tag{11}$$

The effective lateral compressibility modulus of the hybrid composite plate is given as:

$$K_L = K_m + \frac{V_f}{\dfrac{1}{k_f-k_m+\frac{1}{3}\left(G_f-G_m\right)}+\dfrac{1-V_f}{k_m+\frac{4}{3}G_m}} \tag{12}$$

Finally, the effective transversal Young's modulus of the hybrid composite plate is given as follows:

$$E_2 = \frac{2}{\dfrac{1}{2K_L}+\dfrac{1}{2G_{23}}\dfrac{2\left(\nu_{12}\right)^2}{E_1}} \tag{13}$$

3. Formulation of the refined plate theory for hybrid composite lamina

3.1 Kinematics and constitutive equations

We consider a rectangular plate of total thickness h composed of N_p orthotropic layers with the coordinate system shown in Fig. 1.

The displacement field for the refined plate theory is given by the following equations:

$$\begin{cases} u(x,y,z,t) = u_0(x,y,t) - z\dfrac{\partial w_b}{\partial x} - f(z)\dfrac{\partial w_s}{\partial x} \\ v(x,y,z,t) = v_0(x,y,t) - z\dfrac{\partial w_b}{\partial y} - f(z)\dfrac{\partial w_s}{\partial y} \\ w(x,y,z,t) = w_b(x,y,t) + w_s(x,y,t) \end{cases} \tag{14}$$

where $u_0(x, y, t)$ and $v_0(x, y, t)$ are displacement functions of the mid-plane of the plate in the x and y directions,

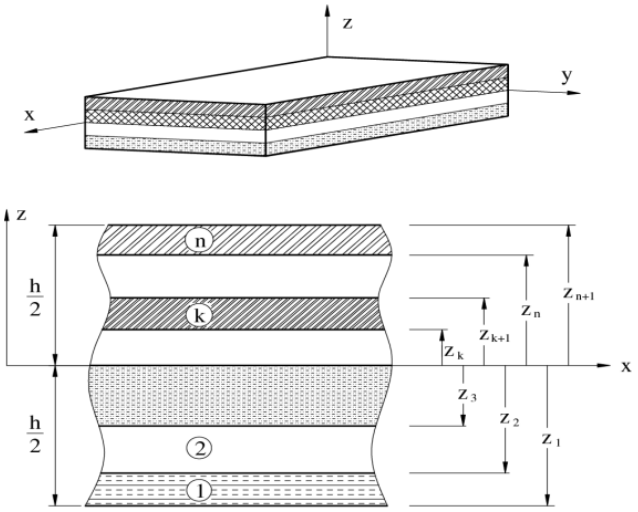

Fig. 1 Coordinate system and layer numbering used for laminated plates

respectively; w_b and w_s are the bending and shear components of transverse displacement, respectively.

The shape function determining the distribution of the transverse shear strains and stresses through the thickness is considered in this paper as:

$$f(z)=\left(z-ze^{\frac{-2z^2}{h^2}}\right) \tag{15}$$

This function ensures zero transverse shear stresses at the top and bottom surfaces of the plate.

The strains associated with the displacement field given in equation (14) are:

$$\begin{cases}\varepsilon_x=\varepsilon_x^0+zk_x^b+f(z)k_x^s=\dfrac{\partial u}{\partial x}-z\dfrac{\partial^2 w_b}{\partial x^2}-f(z)\dfrac{\partial^2 w_s}{\partial x^2}\\ \varepsilon_y=\varepsilon_y^0+zk_y^b+f(z)k_y^s=\dfrac{\partial v}{\partial y}-z\dfrac{\partial^2 w_b}{\partial y^2}-f(z)\dfrac{\partial^2 w_s}{\partial y^2}\\ \gamma_{xy}=\gamma_{xy}^0+zk_{xy}^b+f(z)k_{xy}^s=\dfrac{\partial u}{\partial y}+\dfrac{\partial v}{\partial x}-2z\dfrac{\partial^2 w_b}{\partial x\partial y}-2f(z)\dfrac{\partial^2 w_s}{\partial x\partial y}\\ \gamma_{yz}=g(z)\gamma_{yz}^s=\left(1-\dfrac{df(z)}{dz}\right)\dfrac{\partial w_s}{\partial y}\\ \gamma_{xz}=g(z)\gamma_{xz}^s=\left(1-\dfrac{df(z)}{dz}\right)\dfrac{\partial w_s}{\partial x}\end{cases} \tag{16}$$

For each layer, the strains are related to the stresses through the Hooke's law:

$$\begin{Bmatrix}\sigma_x\\ \sigma_y\\ \tau_{xy}\\ \tau_{yz}\\ \tau_{xz}\end{Bmatrix}=\begin{bmatrix}Q_{11}&Q_{12}&0&0&0\\ Q_{12}&Q_{22}&0&0&0\\ 0&0&Q_{66}&0&0\\ 0&0&0&Q_{44}&0\\ 0&0&0&0&Q_{55}\end{bmatrix}\begin{Bmatrix}\varepsilon_x\\ \varepsilon_y\\ \gamma_{xy}\\ \gamma_{yz}\\ \gamma_{xz}\end{Bmatrix} \tag{17a}$$

where Q_{ij} are the material constants in the material axes of the layer given as:

$$Q_{11}=\frac{E_1}{1-\nu_{12}\nu_{21}},\ Q_{12}=\frac{\nu_{12}E_2}{1-\nu_{12}\nu_{21}},\ Q_{22}=\frac{E_2}{1-\nu_{12}\nu_{21}},\quad Q_{66}=G_{12},\ Q_{44}=G_{23},\ Q_{55}=G_{13} \tag{17b}$$

3.2 Governing equations

The strain energy of the plate can be written as:

$$\begin{aligned}U&=\frac{1}{2}\int_V\sigma_{ij}\varepsilon_{ij}dV\\ &=\frac{1}{2}\int_V\left(\sigma_x\varepsilon_x+\sigma_y\varepsilon_y+\sigma_{xy}\gamma_{xy}+\sigma_{yz}\gamma_{yz}+\sigma_{xz}\gamma_{xz}\right)dV\end{aligned} \tag{18}$$

Substituting equation (16) into equation (18) and integrating through the thickness of the plate, the strain energy of the plate can be rewritten as:

$$\begin{aligned}U=\frac{1}{2}\int_A\big(&N_x\varepsilon_x^0+N_y\varepsilon_y^0+N_{xy}\gamma_{xy}^0+M_x^bk_x^b+M_y^bk_y^b+M_{xy}^bk_{xy}^b+M_x^sk_x^s+M_y^sk_y^s+M_{xy}^sk_{xy}^s\\ &+Q_{yz}^s\gamma_{yz}+Q_{xz}^s\gamma_{xz}\big)dxdy\end{aligned} \tag{19}$$

where N_i, M_i, and Q_i are the stress resultants given by the following integrations:

$$\begin{cases}\left(N_i,M_i^b,M_i^s\right)=\displaystyle\int_{-h/2}^{h/2}\sigma_i\left(1,z,f(z)\right)dz=\\ \displaystyle\sum_{k=1}^{N_p}\int_{z_k}^{z_{k+1}}\sigma_i\left(1,z,f(z)\right)dz,\quad (i=1,2,6)\\ Q_i^s=\displaystyle\int_{-h/2}^{h/2}\sigma_ig(z)dz=\sum_{k=1}^{N_p}\int_{z_k}^{z_{k+1}}\sigma_ig(z)dz,\quad (i=4,5)\end{cases} \tag{20}$$

The kinetic energy of the plate can be written as:

$$\begin{aligned}K=\frac{1}{2}\int_V\rho\ddot{u}_{ii}dV=\frac{1}{2}\int_A\Bigg\{&\delta u_0\left(I_1\ddot{u}_0-I_2\frac{\partial\ddot{w}_b}{\partial x}-I_4\frac{\partial\ddot{w}_s}{\partial x}\right)+\delta v_0\left(I_1\ddot{v}_0-I_2\frac{\partial\ddot{w}_b}{\partial y}-I_4\frac{\partial\ddot{w}_s}{\partial y}\right)\\ &+\delta w_b\left[I_1\left(\ddot{w}_b+\ddot{w}_s\right)+I_2\left(\frac{\partial\ddot{u}_0}{\partial x}+\frac{\partial\ddot{v}_0}{\partial y}\right)-I_3\left(\frac{\partial^2\ddot{w}_b}{\partial x^2}+\frac{\partial^2\ddot{w}_b}{\partial y^2}\right)-I_5\left(\frac{\partial^2\ddot{w}_s}{\partial x^2}+\frac{\partial^2\ddot{w}_s}{\partial y^2}\right)\right]\\ &+\delta w_s\left[I_1\left(\ddot{w}_b+\ddot{w}_s\right)+I_4\left(\frac{\partial\ddot{u}_0}{\partial x}+\frac{\partial\ddot{v}_0}{\partial y}\right)-I_5\left(\frac{\partial^2\ddot{w}_b}{\partial x^2}+\frac{\partial^2\ddot{w}_b}{\partial y^2}\right)-I_6\left(\frac{\partial^2\ddot{w}_s}{\partial x^2}+\frac{\partial^2\ddot{w}_s}{\partial y^2}\right)\right]\Bigg\}dxdy\end{aligned} \tag{21}$$

where ρ is the density of the composite plate and I_i are the inertia terms defined by the following integrations:

$$I_i=\int_{-h/2}^{h/2}\rho\left(1,z,z^2,f(z),zf(z),\left[f(z)\right]^2\right)dz,\qquad (i=1-6) \tag{22}$$

In order to derive the equations of motion of the composite plate, the Hamilton's principle is used:

$$\int_0^t\delta(U-K)\,dt=0 \tag{23}$$

Substituting equations (19) and (21) into equation (23), integrating the obtained equation by parts, and collecting the coefficients of δu_0, δv_0, δw_b and δw_s, the equation of motion of the laminate plate are obtained as:

$$\begin{cases}\delta u_0:\dfrac{\partial N_x}{\partial x}+\dfrac{\partial N_{xy}}{\partial y}=I_1\ddot{u}_0-I_2\dfrac{\partial\ddot{w}_b}{\partial x}-I_4\dfrac{\partial\ddot{w}_s}{\partial x}\\ \delta v_0:\dfrac{\partial N_{xy}}{\partial x}+\dfrac{\partial N_y}{\partial y}=I_1\ddot{v}_0-I_2\dfrac{\partial\ddot{w}_b}{\partial y}-I_4\dfrac{\partial\ddot{w}_s}{\partial y}\\ \delta w_b:\dfrac{\partial^2M_x^b}{\partial x^2}+2\dfrac{\partial^2M_{xy}^b}{\partial x\partial y}+\dfrac{\partial^2M_y^b}{\partial y^2}=I_1\left(\ddot{w}_b+\ddot{w}_s\right)+I_2\left(\dfrac{\partial\ddot{u}_0}{\partial x}+\dfrac{\partial\ddot{v}_0}{\partial y}\right)\\ \qquad\qquad -I_3\left(\dfrac{\partial^2\ddot{w}_b}{\partial x^2}+\dfrac{\partial^2\ddot{w}_b}{\partial y^2}\right)-I_5\left(\dfrac{\partial^2\ddot{w}_s}{\partial x^2}+\dfrac{\partial^2\ddot{w}_s}{\partial y^2}\right)\\ \delta w_s:\dfrac{\partial^2M_x^s}{\partial x^2}+2\dfrac{\partial^2M_{xy}^s}{\partial x\partial y}+\dfrac{\partial^2M_y^s}{\partial y^2}+\dfrac{\partial Q_{xz}^s}{\partial x}+\dfrac{\partial Q_{yz}^s}{\partial y}=I_1\left(\ddot{w}_b+\ddot{w}_s\right)+I_4\left(\dfrac{\partial\ddot{u}_0}{\partial x}+\dfrac{\partial\ddot{v}_0}{\partial y}\right)\\ \qquad\qquad -I_5\left(\dfrac{\partial^2\ddot{w}_b}{\partial x^2}+\dfrac{\partial^2\ddot{w}_b}{\partial y^2}\right)-I_6\left(\dfrac{\partial^2\ddot{w}_s}{\partial x^2}+\dfrac{\partial^2\ddot{w}_s}{\partial y^2}\right)\end{cases} \tag{24}$$

The equation of motion can also be expressed in terms of the displacements (u_0, v_0, w_b, w_s) by substituting the stress resultants from equation (20) in equation (24).

3.3 Exact solutions for an antisymmetric cross-ply hybrid laminates under different boundary condition

For antisymmetric cross-ply laminates, we have the following relationships between plate stiffnesses:

$$\begin{cases} A_{16}=A_{26}=D_{16}=D_{26}=D_{16}^{s}=D_{26}^{s}=H_{16}^{s}=H_{26}^{s}=0 \\ B_{12}=B_{26}=B_{16}=B_{66}=B_{12}^{s}=B_{16}^{s}=B_{26}^{s}=B_{66}^{s}=A_{45}^{s}=0 \\ B_{22}=-B_{11},\ B_{22}^{s}=-B_{11}^{s} \end{cases} \tag{25}$$

The exact solution of equations (24) for the antisymmetric cross-ply laminated plate under various boundary conditions can be constructed according to Adim *et al*. (2016). The boundary conditions for an arbitrary edge with clamped and simply supported edges are:

Clamped (C)

$$u=v=w_b=w_s=\frac{\partial w_b}{\partial x}=\frac{\partial w_b}{\partial y}=\frac{\partial w_s}{\partial x}=\frac{\partial w_s}{\partial y}=0 \tag{26}$$

at $x=0,a$ and $y=0,b$

Simply supported (S)

$$\begin{cases} v=w_b=w_s=\dfrac{\partial w_b}{\partial y}=\dfrac{\partial w_s}{\partial y}=0 \ \text{ at } \ x=0,a \\ u=w_b=w_s=\dfrac{\partial w_b}{\partial x}=\dfrac{\partial w_s}{\partial x}=0 \ \text{ at } \ y=0,b \end{cases} \tag{27}$$

The boundary conditions in Eq. (26) and (27) are satisfied by the following expansions:

$$\begin{cases} u=U_{mn}X_m^{'}(x)Y_n(y)e^{i\omega t} \\ v=V_{mn}X_m(x)Y_n^{'}(y)e^{i\omega t} \\ w_b=W_{bmn}X_m(x)Y_n(y)e^{i\omega t} \\ w_s=W_{smn}X_m(x)Y_n(y)e^{i\omega t} \end{cases} \tag{28}$$

where U_{mn}, V_{mn}, W_{bmn} and W_{smn} unknown parameters that should be determined, ω is the Eigen frequency associated with the (m,n) Eigen-mode and ()' denotes the derivative with respect to the corresponding coordinate. The functions $X_m(x)$ and $Y_n(x)$ are proposed to satisfy at least the geometric boundary conditions given in equations (26) and (27) and represent he approximate shapes of the deflected surface of the plate. These functionsare listed in Table 1 for the different boundary conditions cases with $\lambda = m\pi/a$ and $\mu = n\pi/b$.

Substituting Eqs. (28) and (25) into Eq. (24), the exact solution of antisymmetric cross-ply laminates can be determined from the following equations:

$$\left(\begin{bmatrix} a_{11} & a_{12} & a_{13} & a_{14} \\ a_{12} & a_{22} & a_{23} & a_{24} \\ a_{13} & a_{23} & a_{33} & a_{34} \\ a_{14} & a_{24} & a_{34} & a_{44} \end{bmatrix} - \omega^2 \begin{bmatrix} m_{11} & 0 & m_{13} & m_{14} \\ 0 & m_{22} & m_{23} & m_{24} \\ m_{31} & m_{32} & m_{33} & m_{34} \\ m_{41} & m_{42} & m_{34} & m_{44} \end{bmatrix}\right) \begin{Bmatrix} U_{mn} \\ V_{mn} \\ W_{bmn} \\ W_{smn} \end{Bmatrix} = \begin{Bmatrix} 0 \\ 0 \\ 0 \\ 0 \end{Bmatrix} \tag{29}$$

where:

$$a_{11}=\int_0^a\int_0^b \left(A_{11}X_m^{''}Y_n+A_{66}X_m^{'}Y_n^{'}\right)X_m^{'}Y_n\,dxdy$$

$$a_{12}=\int_0^a\int_0^b (A_{12}+A_{66})X_m^{'}Y_n^{''}X_m^{'}Y_n\,dxdy$$

$$a_{13}=-\int_0^a\int_0^b \left[B_{11}X_m^{''}Y_n+\left(B_{12}+2B_{66}\right)X_m^{'}Y_n^{''}\right]X_m^{'}Y_n\,dxdy$$

$$a_{14}=-\int_0^a\int_0^b \left[B_{11}^{s}X_m^{''}Y_n+\left(B_{12}^{s}+2B_{66}^{s}\right)X_m^{'}Y_n^{''}\right]X_m^{'}Y_n\,dxdy$$

$$a_{21}=\int_0^a\int_0^b (A_{12}+A_{66})X_m^{''}Y_n^{'}X_m^{'}Y_n^{'}\,dxdy$$

$$a_{22}=\int_0^a\int_0^b \left(A_{22}X_mY_n^{'''}+A_{66}X_m^{''}Y_n^{'}\right)X_mY_n^{'}\,dxdy$$

$$a_{23}=-\int_0^a\int_0^b \left[B_{22}X_mY_n^{'''}+\left(B_{12}+2B_{66}\right)X_m^{''}Y_n^{'}\right]X_mY_n^{'}\,dxdy$$

$$a_{24}=-\int_0^a\int_0^b \left[B_{22}^{s}X_mY_n^{'''}+\left(B_{12}^{s}+2B_{66}^{s}\right)X_m^{''}Y_n^{'}\right]X_mY_n^{'}\,dxdy$$

$$a_{31}=\int_0^a\int_0^b \left[B_{11}X_m^{'''}Y_n+\left(B_{12}+2B_{66}\right)X_m^{''}Y_n^{''}\right]X_mY_n\,dxdy$$

$$a_{32}=\int_0^a\int_0^b \left[B_{22}X_mY_n^{''''}+\left(B_{12}+2B_{66}\right)X_m^{''}Y_n^{''}\right]X_mY_n\,dxdy$$

$$a_{33}=\int_0^a\int_0^b -\left[D_{11}X_m^{'''}Y_n+2(D_{12}+2D_{66})X_m^{''}Y_n^{''}+D_{22}X_mY_n^{''''}\right]X_mY_n\,dxdy$$

$$a_{34}=\int_0^a\int_0^b -\left[D_{11}^{s}X_m^{'''}Y_n+2\left(D_{12}^{s}+2D_{66}^{s}\right)X_m^{''}Y_n^{''}+D_{22}^{s}X_mY_n^{''''}\right]X_mY_n\,dxdy$$

$$a_{41}=\int_0^a\int_0^b \left[B_{11}^{s}X_m^{'''}Y_n+\left(B_{12}^{s}+2B_{66}^{s}\right)X_m^{''}Y_n^{''}\right]X_mY_n\,dxdy$$

$$a_{42}=\int_0^a\int_0^b \left[B_{22}^{s}X_mY_n^{''''}+\left(B_{12}^{s}+2B_{66}^{s}\right)X_m^{''}Y_n^{''}\right]X_mY_n\,dxdy$$

$$a_{43}=\int_0^a\int_0^b -\left[D_{11}^{s}X_m^{'''}Y_n+2\left(D_{12}^{s}+2D_{66}^{s}\right)X_m^{''}Y_n^{''}+D_{22}^{s}X_mY_n^{''''}\right]X_mY_n\,dxdy$$

$$a_{44}=\int_0^a\int_0^b -\left[H_{11}^{s}X_m^{'''}Y_n+2\left(H_{12}^{s}+2H_{66}^{s}\right)X_m^{''}Y_n^{''}+H_{22}^{s}X_mY_n^{''''}-A_{55}^{s}X_m^{''}Y_n-A_{44}^{s}X_mY_n^{''}\right]X_mY_n\,dxdy$$

$$m_{11}=\int_0^a\int_0^b -I_1X_m^{'}Y_nX_m^{'}Y_n\,dxdy \qquad m_{14}=\int_0^a\int_0^b I_4X_m^{'}Y_nX_m^{'}Y_n\,dxdy$$

$$m_{22}=\int_0^a\int_0^b -I_1X_mY_n^{'}X_mY_n^{'}\,dxdy \qquad m_{23}=\int_0^a\int_0^b I_2X_mY_n^{'}X_mY_n^{'}\,dxdy$$

$$m_{24}=\int_0^a\int_0^b I_4X_mY_n^{'}X_mY_n^{'}\,dxdy \qquad m_{31}=\int_0^a\int_0^b -I_2X_mY_nX_m^{''}Y_n\,dxdy$$

$$m_{32}=\int_0^a\int_0^b -I_2X_mY_nX_mY_n^{''}\,dxdy$$

$$m_{41}=\int_0^a\int_0^b -I_4X_mY_nX_m^{''}Y_n\,dxdy$$

$$m_{33}=\int_0^a\int_0^b -I_1X_mY_nX_mY_n\,dxdy+\int_0^a\int_0^b I_3X_mY_nX_mY_n^{''}dxdy+\int_0^a\int_0^b I_3X_mY_nX_m^{''}Y_n\,dxdy$$

$$m_{34}=\int_0^a\int_0^b -I_1X_mY_nX_mY_n\,dxdy+\int_0^a\int_0^b I_5X_mY_nX_mY_n^{''}dxdy+\int_0^a\int_0^b I_5X_mY_nX_m^{''}Y_n\,dxdy$$

$$m_{42}=\int_0^a\int_0^b -I_4X_mY_nX_mY_n^{''}dxdy \qquad m_{41}=m_{34}$$

$$m_{44}=\int_0^a\int_0^b -I_1X_mY_nX_mY_n\,dxdy+\int_0^a\int_0^b I_6X_mY_nX_mY_n^{''}dxdy+\int_0^a\int_0^b I_6X_mY_nX_m^{''}Y_n\,dxdy$$

4. Results and discussion

The Navier solution is used in order to determine the natural frequencies of laminated composite plates by solving Eigen value equations (29). Before analysing the free vibration of hybrid composite plates and for verification purpose, the results obtained by the present refined model are compared with existing results in the literature and with numerical results obtained by the finite

Table 1 Admissible functions $X_m(x)$ and $Y_n(y)$

	Boundary conditions		The functions $X_m(x)$ and $Y_n(y)$	
	at $x=0, a$	at $y=0, b$	$X_m(x)$	$Y_n(y)$
SSSS	$X_m(0)=X_m''(0)=0$ $X_m(a)=X_m''(a)=0$	$Y_n(0)=Y_n''(0)=0$ $Y_n(b)=Y_n''(b)=0$	$\sin(\lambda x)$	$\sin(\mu y)$
CCSS	$X_m(0)=X_m'(0)=0$ $X_m(a)=X_m'(a)=0$	$Y_n(0)=Y_n''(0)=0$ $Y_n(b)=Y_n''(b)=0$	$\sin^2(\lambda x)$	$\sin(\mu y)$
CCCC	$X_m(0)=X_m'(0)=0$ $X_m(a)=X_m'(a)=0$	$Y_n(0)=Y_n'(0)=0$ $Y_n(b)=Y_n'(b)=0$	$\sin^2(\lambda x)$	$\sin^2(\mu y)$

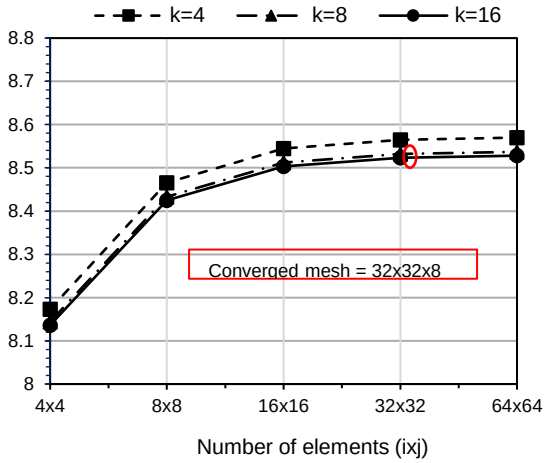

Fig. 2 Convergence of the fundamental frequency for cross-ply antisymmetric $(0°/90°)_1$a square plate with a/h = 5

element method for an antisymmetric cross-ply square laminated plate.

Afterwards, other examples are considered to assess the performance of the present higher-order theory on free vibration analysis of an antisymmetric cross-ply and angle-ply laminated carbon/glass hybrid composite plates.

4.1 Free vibration analysis of cross-ply antisymmetric square laminated plate

The material constants corresponding to the principal material directions are given by Noor (1973):

E_1/E_2 = open, $E_3=E_2$, $G_{12}=G_{13}=0.6E_2$, $G_{23}=0.5E_2$, $\nu_{12}=\nu_{13}=\nu_{23}=0.25$

For convenience, the normalized natural frequencies are used in presenting the results in graphical and tabular forms:

$$\bar{\omega}=\frac{a^2}{h}\sqrt{\frac{\rho}{E_2}} \tag{30}$$

For the finite element simulations with ABAQUS commercial software, for each composite ply a structured $i\times j\times k$ mesh consisting of 8-node linear brick elements (C3D8R) is used. The mesh convergence of the finite element model is shown in Fig. 2. It can be found that with refining meshes, the finite element model converges to a repeatable solution with increasing element number and

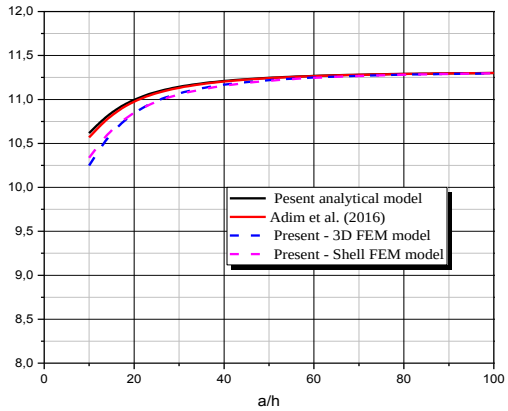

Fig. 3 Fundamental frequencies for simply supported antisymmetric $(0°/90°)_1$ square plate with E_1/E_2=40

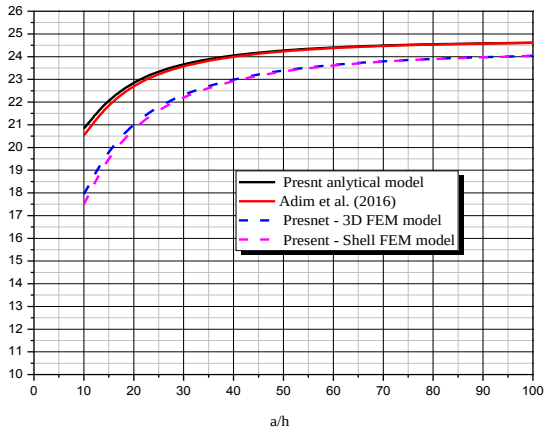

Fig. 4 Fundamental frequencies for clamped antisymmetric $(0°/90°)_1$ square plate with E_1/E_2=40

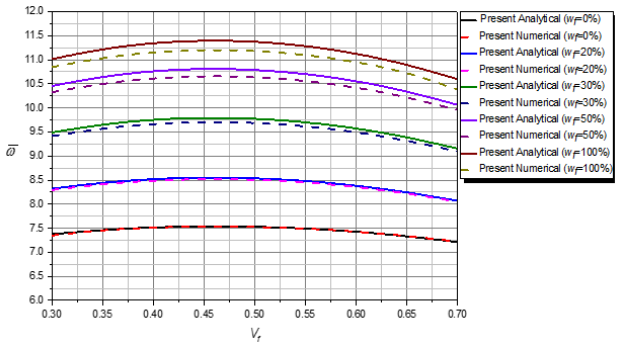

Fig. 5 Effect of fiber volume fraction Vf on the natural frequencies of simply supported antisymmetric cross-ply $(0°/90°)_2$ carbon/glass hybrid square laminated composite plate

additional mesh refinement does not affect results. Considering accuracy and efficiency, 32×32×8 mesh density is used to analyze all examples.

Dimensionless fundamental frequencies of antisymmetric cross-ply $(0°/90°)_n$ square laminates under various thickness ratios a/h and boundary conditions with E_1/E_2 = 40 are shown in Table 2. The obtained results using high-order theory, and those obtained using 3D and shell FEM simulations are compared with available results in the

Table 2 Dimensionless fundamental frequencies of antisymmetric cross-ply square plates for various values of *a*/*h* and different boundary conditions with $E_1/E_2 = 40$

# of layers	a/h	Model	Boundary conditions		
			SSSS	CCSS	CCCC
$(0/90)_1$	10	Present analytical model	10.6164	16.8898	20.8400
		Adim *et al*. (2016a)	10.5680	16.7080	20.5334
		Present 3D FEM	10.2472	14.6323	17.9423
		Present Shell FEM	10.3365	14.3257	17.5049
	20	Present analytical model	11.1188	18.4853	23.4745
		Adim *et al*. (2016a)	11.1052	18.4273	23.3691
		Present 3D FEM	11.0370	17.3592	21.9308
		Present Shell FEM	11.0096	17.2599	21.7838
	50	Present analytical model	11.2773	19.0420	24.4586
		Adim *et al*. (2016a)	11.2751	19.0320	24.4398
		Present 3D FEM	11.2636	18.5627	23.7303
		Present Shell FEM	11.2600	18.5515	23.7124
	100	Present analytical model	11.3007	19.1267	24.6117
		Adim *et al*. (2016a)	11.3002	19.1242	24.6070
		Present 3D FEM	11.2972	18.7630	24.0329
		Present Shell FEM	11.2975	18.7648	24.0347
$(0/90)_3$	10	Present analytical model	15.4885	22.6697	26.5726
		Adim *et al*. (2016a)	15.4632	22.5695	26.3983
		Present 3D FEM	15.2751	19.7506	23.4300
		Present Shell FEM	15.2493	19.5922	23.1887
	20	Present analytical model	17.3840	28.4393	35.2480
		Adim *et al*. (2016a)	17.3772	28.4105	35.1953
		Present 3D FEM	17.3152	26.3303	33.1953
		Present Shell FEM	17.3026	26.2449	32.9779
	50	Present analytical model	18.0655	31.1240	39.9171
		Adim *et al*. (2016a)	18.0644	31.1191	39.9079
		Present 3D FEM	18.1990	30.4203	38.9243
		Present Shell FEM	18.0530	30.2148	38.7421
	100	Present analytical model	18.1701	31.5768	40.7569
		Adim *et al*. (2016a)	18.1698	31.5756	40.7546
		Present 3D FEM	19.2623	31.7414	40.5844
		Present Shell FEM	18.1687	30.9692	39.8703

literature (Adim *et al*. 2016). It can be found that the maximum errors of the present FEM simulations relative to the analytical model are less than 10%. This statement is demonstrated in Fig. 3 and Fig. 4 in which the results obtained by the present theory are in good agreement with other theories (Adim *et al*. 2016) and with FEM results for a wide range of values of thickness ratio. Shell and 3D FEM results are equivalent.

4.2 Free vibration analysis of an anti-symmetrically cross-ply and angle-ply laminated hybrid composite plates

This example is considered to evaluate the performance of the present higher-order theory on free vibration analysis of an anti-symmetrically cross-ply and angle-ply laminated hybrid composite plates. The FEM simulations for the remaining cases were run with the S4R shell elements of Abaqus software because it's less CPU time consuming, and as we have seen the 3D FEM and shell FEM are almost

Table 3 Material properties of composite constituents (Berthelot 2012)

Material	E (GPa)	ν
Glass fiber	86	0.22
Carbon fiber	380	0.3
Kevlar fiber	125	0.3
Epoxy matrix	3.45	0.3

Table 4 Volume fraction V_f effect on the natural frequencies of a cross-ply antisymmetric $(0°/90°)_2$ hybrid carbon/glass square laminated composite plate (SSSS) with a/h=20

w_f(%)			V_f					
Carbon	Glass	Model	0.3	0.4	0.45	0.55	0.6	0.7
		Analytical model	7.6778	7.8366	7.8598	7.8050	7.7298	7.4857
0	100	Numerical model	7.6737	7.8313	7.8540	7.8000	7.7253	7.4828
		Error %	0.0534	0.0677	0.07385	0.06415	0.05825	0.0387
		Analytical model	8.2341	8.4318	8.4593	8.3870	8.2905	7.9783
10	90	Numerical model	8.2254	8.4214	8.4490	8.3173	8.2816	7.9720
		Error %	0,1058	0,1235	0,1219	0,8380	0,1075	0,0790
		Analytical model	8.7522	8.9847	9.0165	8.9299	8.8154	8.4448
20	80	Numerical model	8.7391	8.9691	9.0006	8.9149	8.8013	8.4345
		Error %	0.1499	0.1739	0.1766	0.1682	0.1602	0.1221
		Analytical model	9.2377	9.5014	9.5371	9.4381	9.3075	8.8848
30	70	Numerical model	9.2191	9.4797	9.5151	9.4172	9.2884	8.8638
		Error %	0.2017	0.2289	0.2312	0.2219	0.2056	0.2369
		Analytical model	9.6953	9.9873	10.0267	9.9164	9.7713	9.3012
40	60	Numerical model	9.6711	9.9597	9.9982	9.8896	9.7465	9.2821
		Error %	0.2502	0.2771	0.2850	0.2710	0.2544	0.2058
		Analytical model	10.1289	10.4468	10.4894	10.3689	10.2107	9.6971
50	50	Numerical model	10.0989	10.4124	10.4544	10.3357	10.1797	9.6732
		Error %	0.2971	0.3304	0.3348	0.3212	0.3045	0.2471
		Analytical model	10.5414	10.8833	10.9290	10.7991	10.6287	10.0749
60	40	Numerical model	10.5053	10.8418	10.8867	10.7592	10.5914	10.0459
		Error %	0.3436	0.3828	0.3885	0.3708	0.3522	0.2887
		Analytical model	10.9354	11.2995	11.3480	11.2095	11.0278	10.4366
70	30	Numerical model	10.8993	11.2510	11.2985	11.1628	10.9842	10.4024
		Error %	0.3312	0.4311	0.4381	0.4183	0.3969	0.3288
		Analytical model	11.3128	11.6976	11.7488	11.6023	11.4101	10.7839
80	20	Numerical model	11.2640	11.6417	11.6917	11.5482	11.3596	10.7441
		Error %	0.4332	0.4802	0.4884	0.4685	0.4445	0.3704
		Analytical model	11.6752	12.0795	12.1332	11.9798	11.7773	11.1182
90	10	Numerical model	11.6194	12.0159	12.0682	11.9178	11.7198	11.0728
		Error %	0.4802	0.5293	0.5386	0.5202	0.4906	0.4100
		Analytical model	12.0241	12.4467	12.5028	12.3420	12.1308	11.4408
100	0	Numerical model	11.9612	12.3749	12.4298	12.2728	12.0258	11.3898
		Error %	0.5259	0.5802	0.5873	0.5638	0.8731	0.4478

equivalent. So, the results obtained with the present analytical model are compared with those issued from the shell FEM simulations used as reference solutions.

The material properties of the composite constituents used in this study are given in Table 3 (Berthelot 2012).

Table 4 presents the natural frequencies of simply supported antisymmetric (SSSS) cross-ply $(0°/90°)_2$ carbon/glass hybrid square laminated composite plate using the present analytical model for various fiber fraction V_f with a/h = 20. The obtained results are compared with the FEM simulations generated in this study. The results obtained by the present refined model are in very good agreement with those obtained by the FEM simulations. This statement is demonstrated in Fig. 5 in which the maximum errors of the present theory relative to FEM simulations are less than 1%in a wide range of total fiber volume fraction and carbon/glass percentage. This figure shows clearly that the natural frequencies increase with increasing total fiber volume V_f until reaching its maximum at V_f = 0.45. This point represents the optimal volume fraction of fibers needed to reach the maximum natural frequency. We can also notice that the natural frequencies decreases with decreasing percentage of glass fiber (or increasing percentage of carbon fiber). By combining this two types of fibers to obtain hybrid composite, one can fulfill different criteria (resistance, strength, economic…) in different industrial applications.

The dimensionless fundamental frequencies of antisymmetric cross-ply $(0/90)_n$ carbon/glass hybrid square laminated composite plate under different boundary conditions using the proposed model and the FEM simulations are given in Table 5 and Figs. 6 and 7. It can clearly be seen that the results obtained with the present analytical model are in very good agreement with the

Table 5 Dimensionless natural frequencies of an antisymmetric cross-ply carbon/glass hybrid laminated composite square plate under various *a*/*h* ratios

Boundary conditions	layers	a/h	Model	w_f 100% Glass	25% Carbon + 75% Glass	50% Carbon + 50% Glass	75% Carbon + 25% Glass	100% Carbon
SSSS	$(0/90)_2$	10	Analytical model	7.5341	8.7687	9.7804	10.6370	11.3791
			Numerical model	7.5046	8.8455	9.6568	10.4615	11.1510
			Error %	0.4273	-1.0702	1.2794	1.6679	2.0456
		20	Analytical model	7.8486	9.2604	10.4624	11.5184	12.4665
			Numerical model	7.8433	9.4249	10.4279	11.4660	12.3946
			Error %	0.0673	-1.6779	0.3304	0.4570	0.5803
		50	Analytical model	7.9453	9.4158	10.6836	11.8115	12.8370
			Numerical model	7.9497	9.6032	10.6822	11.8072	12.8207
			Error %	-0.0328	-1.9518	0.0130	0.0361	0.1272
		100	Analytical model	7.9595	9.4387	10.7165	11.8554	12.8929
			Numerical model	7.9633	9.6297	10.7203	11.8590	12.8961
			Error %	-0.0474	-1.9831	-0.0358	-0.0308	0.0249
	$(0/90)_3$	10	Analytical model	7.6794	9.0247	10.1158	11.0317	11.8198
			Numerical model	7.6651	8.9692	10.0542	10.9438	11.7050
			Error %	0.1861	0.6188	0.6128	0.8029	0.9812
		20	Analytical model	8.0057	9.5476	10.8512	11.9904	13.0088
			Numerical model	8.0049	9.5405	10.8363	11.9669	12.9755
			Error %	0.0096	0.07434	0.1378	0.1961	0.2567
		50	Analytical model	8.1061	9.7133	11.0911	12.3116	13.4177
			Numerical model	8.1094	9.7163	11.0932	12.3127	13.4176
			Error %	-0.0413	-0.0307	-0.0192	0.0089	0.0007
		100	Analytical model	8.1208	9.7378	11.1268	12.3598	13.4796
			Numerical model	8.1249	9.7424	11.2096	12.3650	13.4848
			Error %	-0.0504	-0.0477	-0.04437	-0.0418	-0.0389
CCCC	$(0/90)_2$	10	Analytical model	14.3249	16.5190	18.0906	19.2851	20.2309
			Numerical model	13.3419	15.3419	16.1991	17.0086	17.6157
			Error %	7.3677	7.8244	11.6765	13.3845	14.8459
		20	Analytical model	15.9438	19.1331	21.6749	23.7949	25.6140
			Numerical model	15.3356	18.5747	20.5353	22.3704	23.9044
			Error %	3.9646	3.0063	5.5491	6.3677	7.1519
		50	Analytical model	16.5159	20.1390	23.1617	25.7963	28.1544
			Numerical model	16.0945	19.9549	22.5602	25.0958	27.3510
			Error %	2.6184	0.9225	2.6661	2.7913	2.9373
		100	Analytical model	16.6032	20.2970	23.4016	26.1278	28.5858
			Numerical model	16.2141	20.1798	22.9029	25.5744	27.9778
			Error %	2.3995	0.5809	2.1775	2.1637	2.1730
	$(0/90)_3$	10	Analytical model	14.6017	16.9594	18.6217	19.8697	20.8483
			Numerical model	13.6793	15.6494	16.9598	17.8976	18.6038
			Error %	6.7426	5.5569	9.7987	11.0189	12.0647
		20	Analytical model	16.2957	19.7485	22.4761	24.7334	26.6577
			Numerical model	15.7071	18.9417	21.4361	23.4565	25.1457
			Error %	3.7476	4.2592	4.8518	5.4439	6.0130
		50	Analytical model	16.8975	20.8341	24.1017	26.9376	29.4673
			Numerical model	16.4762	20.3306	23.5096	26.2542	28.6922
			Error %	2.5572	2.4765	2.5187	2.6028	2.7015
		100	Analytical model	16.9896	21.0054	24.3658	27.3058	29.9494
			Numerical model	16.5968	20.5562	23.8595	26.7442	29.3324
			Error %	2.3663	2.1850	2.1220	2.0997	2.1036

Table 6 Dimensionless natural frequencies of an antisymmetric cross-ply carbon/glass hybrid rectangular laminated c omposite plate under various aspect ratio*a*/*b*with *a*/*h*=20

Boundary conditions	w_f(%)		Model	a/b						
	Carbon	Glass		0.2	0.6	0.8	1	1.2	1.6	2
			Analytical model	4.8258	5.9163	6.5211	7.8487	9.6132	14.3782	20.6219
	0	100	Numerical model	4.8247	5.6157	6.5169	7.8433	9.6048	14.3415	20.5416
			Error %	0.0228	5.3528	0.0644	0.0688	0.0874	0.2559	0.3909
			Analytical model	5.9642	6.7001	7.7282	9.2605	11.3561	17.1046	24.6358
	25	75	Numerical model	5.9550	6.6157	7.7131	9.2419	11.4660	17.0005	24.4038
			Error %	0.1545	1.2757	0.1958	0.2012	-0.9585	0.6123	0.9507
			Analytical model	6.8983	7.6843	8.7546	10.4624	12.8313	19.3636	27.8802
SSSS	50	50	Numerical model	6.8781	7.6558	8.7263	10.4279	12.7743	19.1779	27.4673
			Error %	0.2937	0.3723	0.3243	0.3308	0.4462	0.9683	1.5032
			Analytical model	7.7038	8.5102	9.6868	11.5184	14.1212	21.3064	30.6147
	75	25	Numerical model	7.6711	8.4654	9.6133	11.4660	14.0342	21.0298	30.0064
			Error %	0.4263	0.5292	0.7646	0.4570	0.6199	1.3153	2.0272
			Analytical model	8.4188	9.2503	10.4676	12.4666	15.2743	23.0183	32.9820
	100	0	Numerical model	8.3717	9.1878	10.4076	12.3946	15.1551	22.6458	32.1707
			Error %	-3.9397	0.6802	0.5765	0.5809	0.7865	1.6449	2.5218
			Analytical model	10.7335	11.2152	11.7607	12.6128	13.8429	17.5926	23.0612
	0	100	Numerical model	10.4260	10.8292	11.3323	12.1781	13.3944	17.1589	22.6327
			Error %	2.9493	3.5644	3.7803	3.5695	3.3484	2.5275	1.8933
			Analytical model	13.1323	13.6281	14.2111	15.1521	16.5505	20.9399	27.4363
	25	75	Numerical model	12.6264	13.0026	13.5330	14.4788	15.8842	20.3392	26.8438
			Error %	4.0067	4.8106	5.0107	4.6502	4.1947	2.9534	2.2072
			Analytical model	15.0173	15.5556	16.1877	17.2172	18.7631	23.6683	30.9509
CCSS	50	50	Numerical model	14.3004	14.6731	15.2421	16.2865	17.8622	22.8801	30.1599
			Error %	5.0131	6.0144	6.2039	5.7145	5.0436	3.4449	2.6227
			Analytical model	16.5792	17.1717	17.8565	18.9700	20.6461	25.9825	33.8947
	75	25	Numerical model	15.6467	16.0251	16.6362	17.7754	19.5052	24.9988	32.8911
			Error %	5.9597	7.1550	7.3352	6.7205	5.8492	3.9350	3,0513
			Analytical model	17.9145	18.5667	19.3052	20.4979	22.2907	27.9964	36.4277
	100	0	Numerical model	16.7665	17.1556	17.8102	19.0392	20.9100	26.8156	35.2054
			Error %	6.8470	8.2253	8.3941	7.6616	6.6031	4.4034	3.4719
			Analytical model	10.7558	11.8380	13.3983	15.9439	19.5009	29.2372	41.6356
	0	100	Numerical model	10.4260	11.4139	12.9075	15.3358	18.6904	27.6398	38.8194
			Error %	3.1632	3.7156	3.8024	3.9652	4.3364	5.7793	7.2546
			Analytical model	13.1558	14.3470	16.1457	19.1331	23.3261	34.6824	48.7797
	25	75	Numerical model	12.6264	13.7103	15.4442	18.2707	22.1352	32.1870	44.9426
			Error %	4.1928	4.6439	4.5421	4.7201	5.3801	7.7528	8.5378
			Analytical model	15.0431	16.3522	18.3475	21.6749	26.3345	38.7947	53.9252
CCCC	50	50	Numerical model	14.3004	15.4847	17.4158	20.5353	24.7387	35.4184	47.9426
			Error %	5.1936	5.6023	5.3497	5.5495	6.4506	9.5326	12.4787
			Analytical model	16.6079	18.0331	20.1946	23.7949	28.8139	42.0685	57.8654
	75	25	Numerical model	15.6467	16.9283	19.0253	22.3704	26.8115	37.8682	50.5712
			Error %	6.1431	6.5263	6.1460	6.3678	7.4684	11.0919	14.4236
			Analytical model	17.9462	19.4834	21.7886	25.6140	30.9187	44.7644	60.0068
	100	0	Numerical model	16.7665	18.1412	20.3805	23.9044	28.5172	39.8063	52.5714
			Error %	7.0360	7.3986	6.9090	7.1518	8.4212	12.4556	14.1434

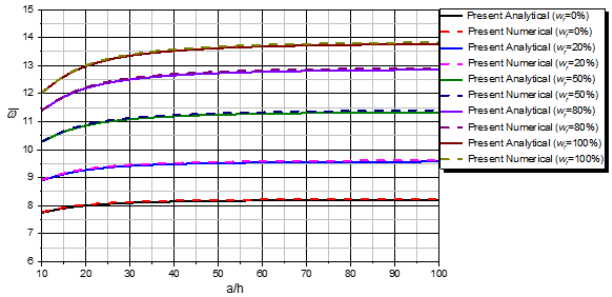

Fig. 6 Effect of the side to thickness ratio a/h on the natural frequencies of an antisymmetric cross-ply $(0/90)_2$ carbon/glass hybrid square laminated composite plate SSSS with V_f =0.5

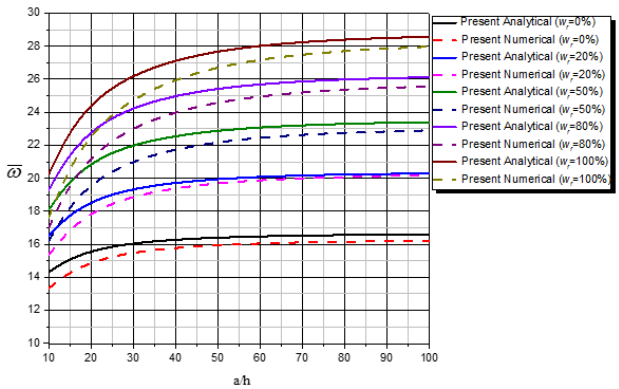

Fig. 7 Effect of the side to thickness ratio a/h on the natural frequencies of an antisymmetric cross-ply $(0/90)_2$ carbon/glass hybrid square laminated composite plate CCCC with V_f =0.5

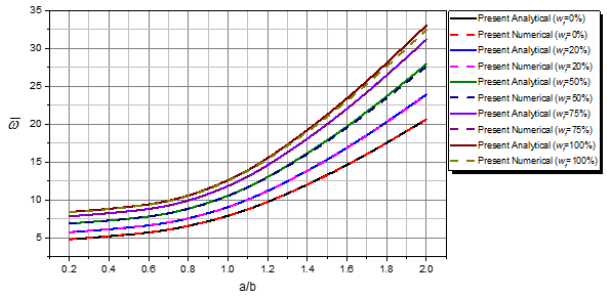

Fig. 8 Effect of aspect ratio a/b on the natural frequencies of an antisymmetric cross-ply $(0/90)_2$ carbon/glass hybrid rectangular laminated composite plate SSSS witha/h =20

corresponding FEM simulations. The maximum errors of the present theory relative to FEM simulations are less than 10%. An increase of the a/h ratio or number of layers lead to the increase of the fundamental frequency and an increase of the carbon fiber percentage (w_f) leads to an increase of the fundamental frequency of the plate for all boundary conditions.

Table 6 and Figs. 8, 9 and 10 show the variation of fundamental frequency with respect to the aspect ratio a/b of an antisymmetric cross-ply (0/90)2 carbon/glass hybrid rectangular laminated composite plate with Vf = 0.5 and a/h = 20 using the proposed model and the FEM simulations. Here again the results obtained with the present analytical

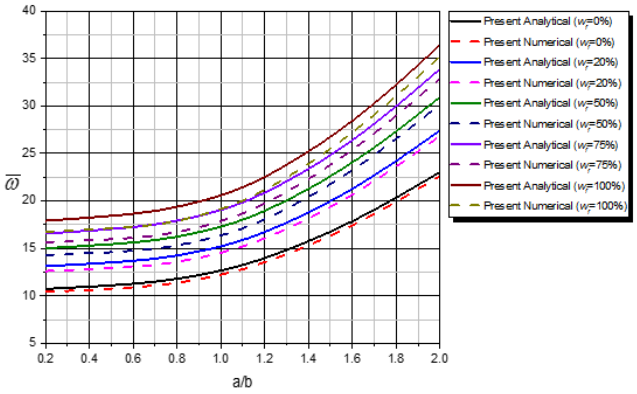

Fig. 9 Effect of the aspect ratio a/b on the natural frequencies of an antisymmetric cross-ply $(0/90)_2$ carbon/glass hybrid rectangular laminated composite plate CCSS with a/h=20

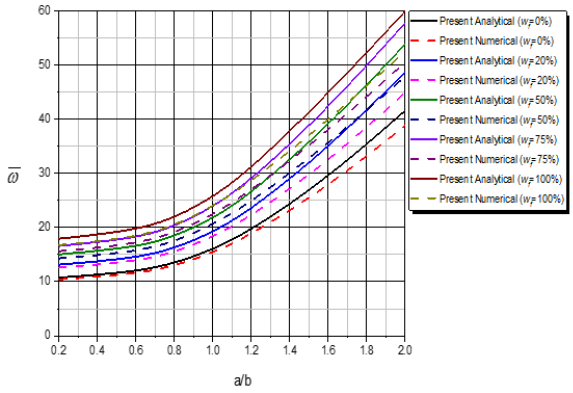

Fig. 10 Effect of aspect ratio a/b on the natural frequencies of an antisymmetric cross-ply $(0/90)_2$ carbon/glass hybrid rectangular laminated composite plate CCCC with a/h =20

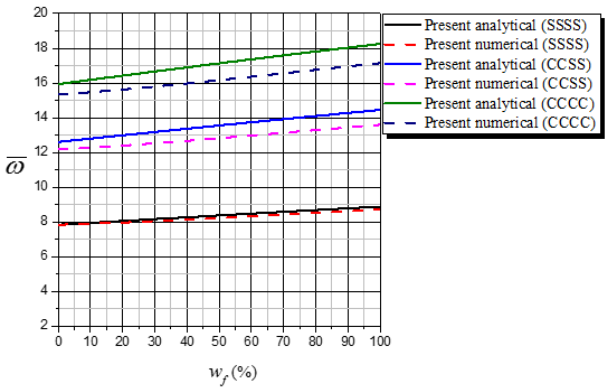

Fig. 11 Effect of fiber percentage w_f on the natural frequencies of an antisymmetric cross-ply $(0/90)_2$ hybrid square laminated composite plate for different boundary conditions with a/h =20

model are in very good agreement with the corresponding FEM simulations. An increase of the a/b ratio and the carbon fiber percentage (wf) lead to an increase of the fundamental frequency of the plate for the different boundary conditions.This means that the plate geometry and the boundary conditions have a very important impact on the stability of the hybrid composite plate.

Table 7 Dimensionless natural frequencies of an antisymmetric cross-ply hybrid square laminated composite plate wi thV_f=0.5anda/h=20

No of layers	w_f(%)		Model	Fiber combinations		
	Material 1	Material 2		Kevlar/Glass	Kevlar/Carbon	Carbon/Glass
SSSS	0	100	Analytical model	7.8487	12.4666	7.8487
			Numerical model	7.8433	12.8028	7.8433
			Error %	0.0685	0.5811	0.0685
	25	75	Analytical model	8.1164	11.6971	9.2605
			Numerical model	7.9984	11.7674	9.2419
			Error %	1.4755	-0.5972	0.2010
	50	50	Analytical model	8.3821	10.8588	10.4624
			Numerical model	8.2306	10.8272	10.4279
			Error %	1.8404	0.2923	0.3304
	75	25	Analytical model	8.6412	9.6411	11.5184
			Numerical model	8.4741	9.8328	11.4660
			Error %	1.9723	-1.9499	0.4570
	100	0	Analytical model	8.8929	8.8929	12.4666
			Numerical model	8.7159	8.7159	12.8028
			Error %	2.0304	2.0304	0.5811
CCSS	0	100	Analytical model	12.6128	20.4979	12.6128
			Numerical model	12.1781	19.0392	12.1781
			Error %	3.5692	7.6617	3.5692
	25	75	Analytical model	13.0927	19.2532	15.1521
			Numerical model	12.4471	18.2078	14.4788
			Error %	5.1866	5.7416	4.6501
	50	50	Analytical model	13.5625	17.8634	17.2172
			Numerical model	12.8269	16.8555	16.2865
			Error %	5.7345	5.9797	5.7146
	75	25	Analytical model	14.0162	16.2864	18.9700
			Numerical model	13.2176	15.3645	17.7754
			Error %	6.0420	6.0003	6.7203
	100	0	Analytical model	14.4535	14.4535	20.4979
			Numerical model	13.6009	13.6009	19.0392
			Error %	6.2688	6.2688	7.6617
CCCC	0	100	Analytical model	15.9439	25.6140	15.9439
			Numerical model	15.3358	23.9034	15.3358
			Error %	3.9652	7.1519	3.9652
	25	75	Analytical model	16.5492	24.1329	19.1331
			Numerical model	15.6823	22.9044	18.2707
			Error %	5.5277	5.3682	4.7198
	50	50	Analytical model	17.1395	22.4574	21.6749
			Numerical model	16.1660	21.2352	20.5353
			Error %	6.0220	5.7554	5.5492
	75	25	Analytical model	17.7077	20.5294	23.7949
			Numerical model	16.6614	19.3748	22.3704
			Error %	6.2801	5.9594	6.3677
	100	0	Analytical model	18.2532	18.2532	25.6140
			Numerical model	17.1461	17.1461	23.9034
			Error %	6.4567	6.4567	7.1519

Table 8 Dimensionless natural frequencies of an antisymmetric cross-ply hybrid square laminated composite plate SSSS with V_f=0.5 and a/h=20

Number of layers	w_f(%)		Theory	Fiber combinations		
	Material 1	Material 2		Kevlar/Glass	Kevlar/Carbon	Carbon/Glass
			Analytical model	7.7298	11.9703	7.7298
	0	100	Numerical model	7.7276	11.9077	7.7276
			Error %	0.0285	0.5257	0,0285
			Analytical model	7.9960	11.3209	9.1129
	25	75	Numerical model	7.9919	11.2720	9.0978
			Error %	0.0513	0.4338	0,1660
			Analytical model	8.2582	10.5869	10.2309
$(0/90)_4$	50	50	Numerical model	8.2519	10.5514	10.2010
			Error %	0.0763	0,3364	0.2931
			Analytical model	8.5119	9.7446	11.1668
	75	25	Numerical model	8.5033	9.7218	11.1208
			Error %	0.1011	0.2345	0.4136
			Analytical model	8.7563	8.7563	11.9703
	100	0	Numerical model	8.7454	8.7454	11.9077
			Error %	0,1246	0.1246	0,5257
			Analytical model	7.7782	12.1139	7.7782
	0	100	Numerical model	7.7827	12.0959	7.7827
			Error %	-0,0578	0,1488	-0,0578
			Analytical model	8.0515	11.4526	9.1967
	25	75	Numerical model	8.0555	11.4403	9.1975
			Error %	-0,0496	0,1075	-0,0087
			Analytical model	8.3206	10.7042	10.3399
$(0/90)_8$	50	50	Numerical model	8.3237	10.6770	10.3358
			Error %	-0.0372	0.2547	0.0397
			Analytical model	8.5807	9.8434	11.2943
	75	25	Numerical model	8.5831	9.8409	11.2844
			Error %	-0.0280	0.0254	0.0877
			Analytical model	8.8312	8.8312	12.1139
	100	0	Numerical model	8.8329	8.8329	12.0959
			Error %	-0.0192	-0.0192	0.1488
			Analytical model	7.7903	12.1495	7.7903
	0	100	Numerical model	7.7965	12.1430	7.7965
			Error %	-0.0795	0.0535	-0.0795
			Analytical model	8.0654	11.4854	9.2183
	25	75	Numerical model	8.0714	11.4824	9.2225
			Error %	-0.0743	0.0261	-0.0455
			Analytical model	8.3361	10.7333	10.3682
$(0/90)_{16}$	50	50	Numerical model	8.3419	10.7335	10.3695
			Error %	-0.0695	-0.0018	-0.0125
			Analytical model	8.5979	9.8680	11.3278
	75	25	Numerical model	8.6034	9.8707	11.3255
			Error %	-0.0639	-0.0273	0.0203
			Analytical model	8.8498	8.8498	12.1495
	100	0	Numerical model	8.8549	8.8549	12.1430
			Error %	-0.0576	-0.0576	0.0535

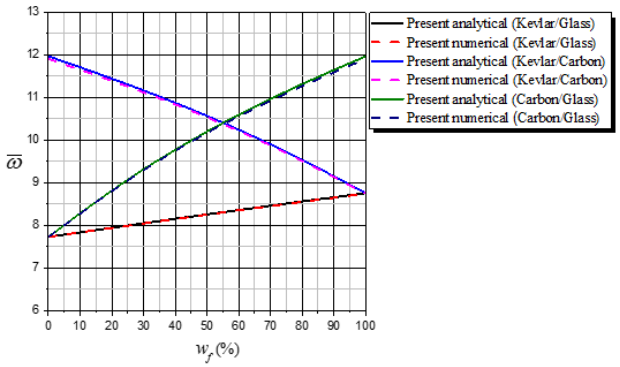

Fig. 12 Effect of fiber percentage w_f on the natural frequencies of an antisymmetric cross-ply $(0/90)_2$ hybrid square laminated composite plate with a/h =20

In the last examples (Tables 7 and 8) and (Figs. 11 and 12), different combinations of fibers and boundary conditions are used in hybrid composite plate with V_f = 0.5 and a/h = 20 using the proposed model and the FEM simulations. The fundamental frequency are minimum for the case of Kevlar/Glass hybrid composite and maximum for the case of Kevlar/Carbon composite.Indeed, the Kevlar/Carbon combination gives the better features of the three combination:the carbon fibers increasethe rigidity to the plate and the Kevlar fibers insure the vibration damping.

5. Conclusions

In this study, a refined shear deformation theory and a finite element method have been successfully used for the free vibration of antisymmetric cross-ply hybrid laminated composite plates under different boundary conditions. The present analytical model supposes the parabolic variation of the transverse shear strains across the plate thickness and satisfies the zero shear stress on the top and bottom surfaces of the plate without need of shear correction factors. The equations of motion were developed using Hamilton's principle. The accuracy and efficiency of the present refined theory was demonstrated for free vibration stability of anti-symmetric cross-ply hybrid laminated composite plates. The natural frequencies predicted by the present theory using just four unknowns are almost identical to those found by the shear deformation theories of five unknowns. The present theory can predict accurately the natural frequencies of hybrid laminated composite plates in a wide range of fibers mixture. It was shown that the fibers combinations affect significantly the fundamental frequencies. It can be concluded that the present models proposed are accurate in solving the vibration behaviors of anti-symmetric cross-ply hybrid laminated composite. Finally, researchers and manufacturers can choose wisely the fiber combinations that give rise to hybrid composite plates that offer rigidity, strength and reduced costs.

Acknowledgments

This research was supported by the French Ministry of Foreign Affairs and International Development (MAEDI) and Ministry of National Education, Higher Education and Research (MENESR) and by the Algerian Ministry of Higher Education and Scientific Research (MESRS) under Grant No. PHC Tassili 17MDU992. Their support is greatly appreciated.

References

Abdelhak, Z., Hadji, L., Khelifa, Z., Hassaine Daouadji, T. and Adda Bedia, E.A. (2016), "Analysis of buckling response of functionally graded sandwich plates using a refined shear deformation theory", *Wind Struct.*, **22**(3), 291-305. https://doi.org/10.12989/was.2016.22.3.291.

Abualnour, M., Houari, M.S.A., Tounsi, A. and Mahmoud, S.R. (2018), "A novel quasi-3D trigonometric plate theory for free vibration analysis of advanced composite plates", *Compos. Struct.*, **184**, 688-697. https://doi.org/10.1016/j.compstruct.2017.10.047.

Abdelaziz, H.H., Meziane, M.A.A., Bousahla, A.A., Tounsi, A., Mahmoud, S.R. and Alwabli, A.S. (2017), "An efficient hyperbolic shear deformation theory for bending, buckling and free vibration of FGM sandwich plates with various boundary conditions", *Steel Compos. Struct.*, **25**(6), 693-704.

Belkacem, A., Tahar, H.D., Abderrezak, R., Amine, B.M., Mohamed, Z. and Boussad, A. (2018), "Mechanical buckling analysis of hybrid laminated composite plates under different boundary conditions", *Struct. Eng. Mech.*, **66**(6), 761-769. https://doi.org/10.12989/sem.2018.66.6.761.

Adim Belkacem, Hassaine Daouadji, T., Rabia Benferhat and Lazreg Hadji, (2016a), "An efficient and simple higher order shear deformation theory for bending analysis of composite plates under various boundary conditions", *Earthq. Struct.*, **11**(1), 63-82. https://doi.org/10.12989/eas.2016.11.1.063.

Adim, B., Hassaine Daouadji, T., Rabia, B. and Hadji, L. (2016b), "Buckling and free vibration analysis of laminated composite plates using an efficient and simple higher order shear deformation theory" *Mech. Industry,* **17**, 512. https://doi.org/10.1051/meca/2015112.

Attia, A., Bousahla, A.A., Tounsi, A., Mahmoud, S.R. and Alwabli, A.S. (2018), "A refined four variable plate theory for thermoelastic analysis of FGM plates resting on variable elastic foundations", *Struct. Eng. Mech.*, **65**(4), 453-464. https://doi.org/10.12989/sem.2018.65.4.453.

Belabed, Z., Bousahla, A.A., Houari, M.S.A., Tounsi, A. and Mahmoud, S.R. (2018), "A new 3-unknown hyperbolic shear deformation theory for vibration of functionally graded sandwich plate", *Earthq. Struct.*, **14**(2), 103-115. https://doi.org/10.12989/eas.2018.14.2.103.

Adim, B., Hassaine Daouadji, T. and Rabahi, A. (2016), "A simple higher order shear deformation theory for mechanical behavior of laminated composite plates", *Int. J. Adv. Struct. Eng.,* **8**, 103-117. https://doi.org/10.1007/s40091-016-0109-x.

Bellifa, H., Bakora, A., Tounsi, A., Bousahla, A.A. and Mahmoud, S.R. (2017), "An efficient and simple four variable refined plate theory for buckling analysis of functionally graded plates", *Steel Compos. Struct.*, **25**(3), 257-270.

Beldjelili, Y., Tounsi, A. and Mahmoud, S.R. (2016), "Hygro-thermo-mechanical bending of S-FGM plates resting on variable elastic foundations using a four-variable trigonometric plate theory", *Smart Strcut. Syst.*, **18**(4), 755-786.

Benhenni Mohamed, Hassaine Daouadji, T., Boussad Abbes, Yu Ming LI , Fazilay Abbes (2018), "Analytical and Numerical Results for Free Vibration of Laminated Composites Plates", *J. Chem. Molecular Eng.*, **12**(6), 300-304.

Benchohra, M., Driz, H., Bakora, A., Tounsi, A., Adda Bedia, E. A. and Mahmoud, S.R. (2018), "A new quasi-3D sinusoidal

shear deformation theory for functionally graded plates", *Struct. Eng. Mech.*, **65**(1), 19-31. https://doi.org/10.12989/sem.2018.65.1.019.

Benferhat, R., Hassaine Daouadji, T. and Said Mansour, M. (2016a), "Free vibration analysis of FG plates resting on the elastic foundation and based on the neutral surface concept using higher order shear deformation theory", *Comptes Rendus de Mécanique*, **344**(9), 631-641. https://doi.org/10.1016/j.crme.2016.03.002.

Benferhat, R., Hassaine, D., Hadji, L. and Said, M. (2016b), "Static analysis of the FGM plate with porosities", *Steel Compos. Struct.*, **21**(1), 123-136. https://doi.org/10.12989/scs.2016.21.1.123.

Bennoun, M. and Tounsi, A. (2016), "A novel five variable refined plate theory for vibration analysis of functionally graded sandwich plates", *Mech. Adv. Mater. Struct*., **23**(4), 423-431. https://doi.org/10.1080/15376494.2014.984088.

Bounouara, F., Benrahou, K.H., Belkorissat, I. and Tounsi, A. (2016), "A nonlocal zeroth-order shear deformation theory for free vibration of functionally graded nanoscale plates resting on elastic foundation", *Steel Compos. Struct*., **20**(2), 227-249. https://doi.org/10.12989/scs.2016.20.2.227.

Boukhari, A., Atmane, H.A., Tounsi, A., Adda, B. and Mahmoud, S.R. (2016), "An efficient shear deformation theory for wave propagation of functionally graded material plates", *Struct. Eng. Mech.*, **57**(5), 837-859. https://doi.org/10.12989/sem.2016.57.5.837.

Bousahla, A.A., Benyoucef, S., Tounsi, A. and Mahmoud, S.R. (2016), "On thermal stability of plates with functionally graded coefficient of thermal expansion", *Struct. Eng. Mech*., **60**(2), 313-335. https://doi.org/10.12989/sem.2016.60.2.313.

Bouderba, B., Houari, M.S.A., Tounsi, A. and Mahmoud, S.R. (2016), "Thermal stability of functionally graded sandwich plates using a simple shear deformation theory", *Struct. Eng. Mech*., **58**(3), 397-422. https://doi.org/10.12989/sem.2016.58.3.397.

Berthelot, J.M. (2012), *Matériaux Composites: Comportement Mécanique et Analyse des Structures*, Lavoisier, Paris, France.

Draiche, K., Tounsi, A. and Mahmoud, S.R. (2016), "A refined theory with stretching effect for the flexure analysis of laminated composite plates", *Geomech. Eng.*, **11**(5), 671-690. https://doi.org/10.12989/gae.2016.11.5.671.

El-Haina, F., Bakora, A., Bousahla, A.A., Tounsi, A. and Mahmoud, S.R. (2017), "A simple analytical approach for thermal buckling of thick functionally graded sandwich plates", *Struct. Eng. Mech*., **63**(5), 585-595. https://doi.org/10.12989/sem.2017.63.5.585.

Fourn, H., Atmane, H.A., Bourada, M., Bousahla, A.A., Tounsi, A. and Mahmoud, S.R. (2018), "A novel four variable refined plate theory for wave propagation in functionally graded material plates", *Steel Compos. Struct.*, **27**(1), 109-122.

Hadji, L., Khelifa, Z. and Adda Bedia, E.A. (2016), "A New Higher Order Shear Deformation Model for Functionally Graded Beams", KSCE Journal of Civil Engineering", **20**(5), 1835-1841. https://doi.org/10.1007/s12205-015-0252-0.

Hadji, L., Zouatnia, N., and Kassoul, A., (2017), "Wave propagation in functionally graded beams using various higher-order shear deformation beams theories" , *Struct. Eng. Mech.*, **62**(2), 143-149.

Hadji, L., Zouatnia, N. and Bernard, F. (2019a), "An analytical solution for bending and free vibration responses of functionally graded beams with porosities: Effect of the micromechanical models", *Struct. Eng. Mech.*, **69**(2), 231-241.

Hadji, L. and Zouatnia, N. (2019b), "Effect of the micromechanical models on the bending of FGM beam using a new hyperbolic shear deformation theory", *Earthq. Struct.*, **16**(2),177-183.

Hassaine Daouadji T. and Adim Belkacem (2017), "Mechanical behaviour of FGM sandwich plates using a quasi-3Dhigher order shear and normal deformation theory", *Struct. Eng. Mech.*, **61**(1), 49-63. https://doi.org/10.12989/sem.2017.61.1.049.

Hassaine Daouadji, T., Benferhat, R. and Belkacem, A. (2016a), "Bending analysis of an imperfect advanced composite plates resting on the elastic foundations", *Coupled Syst. Mech.*, **5**(3), 269-285.

Hassaine Daouadji, T. and Adim Belkacem (2016b), "An analytical approach for buckling of functionally graded plates" *Adv. Mater. Res.*, **5**(3), 141-169. https://doi.org/10.12989/amr.2016.5.3.141.

Houari, M.S.A., Tounsi, A., Bessaim, A. and Mahmoud, S.R. (2016), "A new simple three-unknown sinusoidal shear deformation theory for functionally graded plates", *Steel Compos. Struct*., **22**(2), 257-276. https://doi.org/10.12989/scs.2016.22.2.257.

Javed, S., Viswanathan, K.K., NurulIzyan, M.D., Aziz, Z.A. and Lee, J.H. (2018), "Free vibration of cross-ply laminated plates based on higher-order shear deformation theory", *Steel Compos. Struct.*, **26**(4). https://doi.org/10.12989/scs.2018.26.4.473.

Kaci, A., Houari, M.S.A., Bousahla, A.A., Tounsi, A. and Mahmoud, S.R. (2018), "Post-buckling analysis of shear-deformable composite beams using a novel simple two-unknown beam theory", *Struct. Eng. Mech.*, **65**(5), 621-631. https://doi.org/10.12989/sem.2018.65.5.621.

Karami, B., Janghorban, M., Shahsavari, D. and Tounsi, A. (2018), "A size-dependent quasi-3D model for wave dispersion analysis of FG nanoplates", *Steel Compos. Struct.*, **28**(1), 99-110. https://doi.org/10.12989/scs.2018.28.1.099.

Khalifa, Z., Hadji, L., Hassaine Daouadji, T. and Bourada, M. (2018), "Buckling response with stretching effect of carbon nanotube-reinforced composite beams resting on elastic foundation", *Struct. Eng. Mech.*, **67**(2), 125-130. https://doi.org/10.12989/sem.2018.67.2.125.

Mahi, A., Adda Bedia, E.A. and Tounsi, A. (2015), "A new hyperbolic shear deformation theory for bending and free vibration analysis of isotropic, functionally graded, sandwich and laminated composite plate", *Appl. Math. Model*., **39**(9), 2489-2508. https://doi.org/10.1016/j.apm.2014.10.045.

Mantari, J.L., Oktem, A.S. and Guedes Soares, C. (2012), "A new trigonometric shear deformation theory for isotropic, laminated composite and sandwich plates", *J. Solid Struct.*, **49**, 43-53.

Menasria, A., Bouhadra, A., Tounsi, A., Bousahla, A.A. and Mahmoud, S.R. (2017), "A new and simple HSDT for thermal stability analysis of FG sandwich plates", *Steel Compos. Struct.*, **25**(2), 157-175. https://doi.org/10.12989/scs.2017.25.2.157.

Mindlin, R.D. (1951), "Influence of rotatory inertia and shear on flexural motions of isotropic, elastic plates", ASME *J. Appl. Mech.*, **18**, 31-38.

Noor, A.K. (1973), "Free vibrations of multilayered composite plates", *AIAA J*., **11**(7), 1038-1039.

Benferhat, R., Hassaine Daouadji, T. and Mansour, M.S. (2016a), "Free vibration analysis of FG plates resting on the elastic foundation and based on the neutral surface concept using higher order shear deformation theory", *Comptes Rendus Mecanique*, **344**(9), 631-641. https://doi.org/10.1016/j.crme.2016.03.002.

Benferhat, R., Hassaine Daouadji, T., Mansour, M.S. and Hadji, L. (2016b), "Effect of porosity on the bending and free vibration response of functionally graded plates resting on Winkler-Pasternak foundations", *Earthq. Struct*., **10**(5), 1429-1449. https://doi.org/10.12989/eas.2016.10.6.1429.

Reddy, J.N. (1984a), "A simple higher-order theory for laminated composite plates", *J. Appl. Mech.*, 51, 745-752. https://doi.org/10.1115/1.3167719.

Reddy, J.N. (1984b), "A refined nonlinear theory of plates with transverse shear deformation", *J. Solid Struct.*,20(9/10), 881-896. https://doi.org/10.1016/0020-7683(84)90056-8.

Reddy, J.N. (1990), "A general nonlinear third-order theory of plates with transverse shear deformation", *J. Non-Linear Mech.*, **25**(6), 677-686.

Reddy, J.N. (1997), *Mechanics of Laminated Composite Plates - Theory and Analysis*, CRC Press, New York, NY, USA.

Ren, J.G. (1990), "Bending, vibration and buckling of laminated plates", *Handbook of Ceramics and Composites*, Marcel Dekker, New York, USA.

Stavski, Y. (1965), "On the theory of symmetrically heterogeneous plates having the same thickness variation of the elastic moduli", *Topics Appl. Mech.*, Elsevier, New York, U.S.A.

Sathishkumar, T.P., Naveen, J. and Satheeshkumar, S. (2014), "Hybrid fiber reinforced polymer composites - A review", *J. Reinforced Plastics Compos.*, **33**(5), 454-471. https://doi.org/10.1177/0731684413516393.

Sobhy, M. (2013), "Buckling and free vibration of exponentially graded sandwich plates resting on elastic foundations under various boundary conditions", *Compos. Struct.*, **99**, 76-87. https://doi.org/10.1016/j.compstruct.2012.11.018.

Hassaine Daouadji, T., B. Adim (2016a) "Theoretical analysis of composite beams under uniformly distributed load", *Adv. Mater. Res.*, **5**(1), 1-9. https://doi.org/10.12989/amr.2016.5.1.001.

Hassaine Daouadji, T., Benferhat, R. and Belkacem, A. (2016b), "A novel higher order shear deformation theory based on the neutral surface concept of FGM plate under transverse load", *Adv. Mater. Res.*, **5**(2), 107-120. https://doi.org/10.12989/amr.2016.5.2.107.

Hassaine Daouadji, T., Adim, B. and Benferhat, R. (2016c), "Bending analysis of an imperfect FGM plates under hygro-thermo-mechanical loading with analytical validation", *Adv. Mater. Res.*, **5**(1), 35-53. https://doi.org/10.12989/amr.2016.5.1.035.

Tounsi, A., Houari, M.S.A. and Benyoucef, S. (2013), "A refined trigonometric shear deformation theory for thermoelastic bending of functionally graded sandwich plates", *Aerosp. Sci. Technol.*, **24**(1), 209-220. https://doi.org/10.1016/j.ast.2011.11.009.

Tu, T.M., Quoc, T.H. and Long, N.V. (2017), "Bending analysis of functionally graded plates using new eight-unknown higher order shear deformation theory", *Struct. Eng. Mech.*, **62**(3), 311-324. https://doi.org/10.12989/sem.2017.62.3.311.

Vasiliev, V.V. and Morozov, E.V. (2001), *Mechanics and Analysis of Composite Materials*, Elsevier Science, Oxford, United Kingdom.

Whitney, J.M. (1973), "Shear correction factors for orthotropic laminates under static load", *J. Appl. Mech.*, **40**(1), 302-304. https://doi.org/10.1115/1.3422950.

Yazid, M., Heireche, H., Tounsi, A., Bousahla, A.A. and Houari, M.S.A. (2018), "A novel nonlocal refined plate theory for stability response of orthotropic single-layer graphene sheet resting on elastic medium", *Smart Struct. Syst.*, **21**(1), 15-25.

Younsi, A., Tounsi, A., Zaoui, F.Z., Bousahla, A.A. and Mahmoud, S.R. (2018), "Novel quasi-3D and 2D shear deformation theories for bending and free vibration analysis of FGM plates", *Geomech. Eng.*, **14**(6), 519-532. https://doi.org/10.12989/gae.2018.14.6.519.

Yousfi, M., Ait Atmane, H., Meradjah, M., Tounsi, A. and Bennai, R. (2018), "Free vibration of FGM plates with porosity by a shear deformation theory with four variables", *Struct. Eng. Mech.*, **66**(3), 353-368.

Zenkour, A.M. (2006), "Generalized shear deformation theory for bending analysis of functionally graded plates", *Appl. Math. Model.*, **30**, 67-84. https://doi.org/10.1016/j.apm.2005.03.009.

Abdelhak, Z., Hadji, L., Hassaine Daouadji, T. and Adda Bedia, E.A. (2016), "Thermal buckling response of functionally graded sandwich plates with clamped boundary conditions", *Smart Struct. Syst.*, **18**(2), 267-291. https://doi.org/10.12989/sss.2016.18.2.267.

Zouatnia, N., Hadji, L. and Kassoul, A. (2018), "An efficient and simple refined theory for free vibration of functionally graded plates under various boundary conditions", *Geomech. Eng.*, **16**(1), 1-9. https://doi.org/10.12989/gae.2018.16.1.001.

CC